

Preparation and Properties of a Monomeric High-Spin Mn^V–Oxo Complex

Taketo Taguchi,[†] Rupal Gupta,[‡] Benedikt Lassalle-Kaiser,[§] David W. Boyce,^{||} Vittal K. Yachandra,[§] William B. Tolman,^{*,||} Junko Yano,^{*,§} Michael P. Hendrich,^{*,‡} and A. S. Borovik^{*,†}

[†]Department of Chemistry, University of California-Irvine, 1102 Natural Sciences II, Irvine, California 92697, United States

[‡]Department of Chemistry, Carnegie Mellon University, Pittsburgh, Pennsylvania 15213, United States

[§]Physical Biosciences Division, Lawrence Berkeley National Laboratory, Berkeley, California 94720, United States

^{||}Department of Chemistry and Center for Metals in Biocatalysis, University of Minnesota, Minneapolis, Minnesota 55455, United States

S Supporting Information

ABSTRACT: Oxomanganese(V) species have been implicated in a variety of biological and synthetic processes, including their role as a key reactive center within the oxygen-evolving complex in photosynthesis. Nearly all mononuclear Mn^V–oxo complexes have tetragonal symmetry, producing low-spin species. A new high-spin Mn^V–oxo complex that was prepared from a well-characterized oxomanganese(III) complex having trigonal symmetry is now reported. Oxidation experiments with [FeCp₂]⁺ were monitored with optical and electron paramagnetic resonance (EPR) spectroscopies and support a high-spin oxomanganese(V) complex formulation. The parallel-mode EPR spectrum has a distinctive *S* = 1 signal at *g* = 4.01 with a six-line hyperfine pattern having *A_z* = 113 MHz. The presence of an oxo ligand was supported by resonance Raman spectroscopy, which revealed O-isotope-sensitive peaks at 737 and 754 cm⁻¹ assigned as a Fermi doublet centered at 746 cm⁻¹ ($\Delta^{18}\text{O} = 31 \text{ cm}^{-1}$). Mn *K* β X-ray emission spectra showed *K* β' and *K* $\beta_{1,3}$ bands at 6475.92 and 6490.50 eV, respectively, which are characteristic of a high-spin Mn^V center.

Manganese–oxo complexes have prominent roles in several chemical and biological processes.¹ In biology, high-valent Mn–oxo species may be consequential in the oxidation of water to dioxygen within the photosynthetic membrane protein (Photosystem II, PSII).² Catalysis occurs at the oxygen-evolving complex (OEC) in PSII, which contains a Mn₄Ca cluster surrounded by a network of H-bonds. The structure of the cluster can be described as a Mn₃CaO₄ distorted cube with an oxo-bridged external manganese center.³ The mechanism of water oxidation is still debated, yet one common proposal invokes the generation of high-valent Mn species prior to the formation of the O–O bond.⁴ In this premise, photooxidation would produce a high-energy transient state (*S*₄) containing Mn^V–oxo and Ca^{II}–OH centers that initially couple to form a peroxo intermediate and, ultimately, dioxygen (Figure 1).

The properties of a Mn^V–oxo center that can lead to O–O bond formation are unknown, leading to efforts to prepare

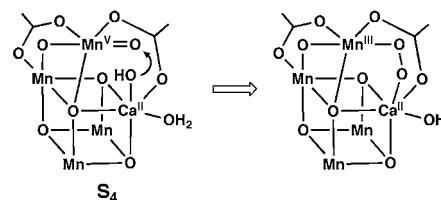


Figure 1. Hypothetical representation of the *S*₄ state in the OEC and a possible route to the formation of the O–O bond.

synthetic systems that probe this process. Some successes have been reported, including the work of Nam and Åkermark,⁵ who showed that dioxygen can be produced from Mn(V)–O species and hydroxide ions. In addition to water oxidation, Mn^V–oxo complexes have been invoked as oxidants in O-atom transfer reactions and C–H bond functionalization.⁶ Most of these complexes contain ancillary porphyrin,⁷ corrole,⁸ corrolazine,⁹ or salen ligands,¹⁰ producing species that are low-spin with *S* = 0 spin ground states. This observation follows from the established theory that predicts that *all* tetragonal d² metal–oxo complexes will be diamagnetic, resulting in a triple bond between the metal center and the terminal oxo ligand (Figure 2A).¹¹ Results from the few characterized tetragonal Mn^V–oxo species support this prediction, insofar as the observed spectroscopic and structural properties indicate the existence of a low-spin Mn≡O unit.¹²

The lone Mn^V–oxo site in the OEC could also be high-spin (*S* = 1). Less is known about the chemistry of metal–oxo complexes in this spin state: we are aware of only one report concerning a high-spin Mn^V–oxo complex, a Mn^V(O)–porphyrin species for which only a room-temperature magnetic moment was used to evaluate its magnetic properties.¹³ In addition, an isoelectronic Mn^V–imido complex has been prepared,¹⁴ the properties of which suggested that it is paramagnetic. One approach toward preparing high-spin metal–oxo species is to enforce local trigonal symmetry within the complex. Mayer and Thorn¹⁵ were the first to suggest that metal–oxo complexes with trigonal symmetry possess two low-

Received: November 21, 2011

Published: January 10, 2012

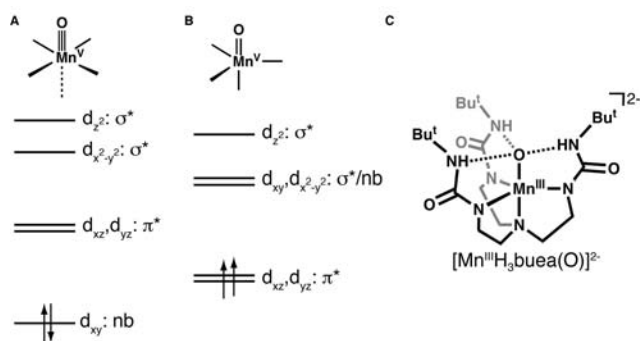


Figure 2. (A, B) Qualitative orbital splitting diagrams for oxometal complexes with (A) tetragonal^{11a} and (B) trigonal¹⁵ symmetries. (C) Structure of the oxomanganese(III) precursor.

lying degenerate orbitals that produce $S = 1$ spin ground states for d^2 metal–oxo complexes (Figure 2B).¹⁶ This theoretical prediction suggests that the metal–oxo interactions in such complexes are weaker than those with tetragonal symmetry, making the former a more reactive species.

This report describes the preparation and spectroscopic properties of a high-spin Mn^V –oxo complex in which the oxo ligand arises from H_2O . The complex is supported by the ligand tris[(*N'*-*tert*-butylureaylato)-*N*-ethylene]aminato ($[H_3buea]^{3-}$), which promotes C_3 molecular symmetry and influences the secondary coordination sphere through an intramolecular H-bonding network around the Mn^V –oxo unit. Our findings demonstrate the feasibility of high-spin Mn^V –oxo complexes and provide a spectroscopic framework for probing their role in chemical processes.

We previously synthesized $[Mn^{III}H_3buea(O)]^{2-}$, the only example of a monomeric Mn^{III} –oxo complex (Figure 2C).¹⁷ Unlike most monomeric metal–oxo complexes, there are three intramolecular H-bonds between the oxo ligand and $[H_3buea]^{3-}$ that aid in the isolation of the complex. $[Mn^{III}H_3buea(O)]^{2-}$ has unusually low oxidation potentials because of the highly anionic ligand field surrounding the manganese center, making it a convenient synthon for the preparation of higher-valent Mn –oxo species. We showed that the one-electron oxidation of $[Mn^{III}H_3buea(O)]^{2-}$ to its Mn^{IV} –oxo derivative at room temperature in DMSO can be accomplished at -1.0 V vs $[FeCp_2]^{+/0}$ (-0.34 V vs NHE).¹⁸ A second oxidative process was observed at -0.076 V vs $[FeCp_2]^{+/0}$ ($+0.59$ V vs NHE), which we assigned to the $Mn^{V/IV}$ –oxo redox couple. However, this process was reversible only at the relatively fast scan rate of 50 V/s, which hindered further characterization of this oxidized species at room temperature. We have found that measuring the redox potential at -60 °C in DMF produces a quasi-reversible one-electron redox process at -0.08 V vs $[FeCp_2]^{+/0}$ at a significantly lower scan rate of 0.100 V/s (Figure S1 in the Supporting Information), suggesting the possibility of detecting this putative Mn^V –oxo species at lower temperatures.

The sequential oxidation of $[Mn^{III}H_3buea(O)]^{2-}$ (Scheme 1) was followed spectrophotometrically at -80 °C in 1:1 THF/

Scheme 1



Conditions: (a) 1.0 equiv $[FeCp_2]^+$, 1:1 DMF/THF, -80 °C; (b) 1–1.5 equiv $[FeCp_2]^+$, 1:1 DMF/THF, -80 °C

DMF (Figure 3A). The optical properties of $[Mn^{III}H_3buea(O)]^{2-}$ at $\lambda_{max} = 710$ and 500 nm disappeared

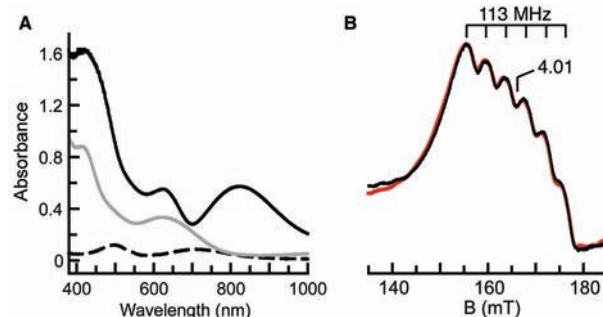


Figure 3. (A) Electronic absorption spectra of $[Mn^{III}H_3buea(O)]^{2-}$ (dashed), $[Mn^{IV}H_3buea(O)]^-$ (solid gray), and $[Mn^VH_3buea(O)]$ (solid black) collected at -80 °C in 1:1 THF/DMF. (B) ||-mode EPR spectrum of $[Mn^VH_3buea(O)]$ (black) and simulated spectrum (red). See Figure 4 for the experimental conditions.

upon the addition of 1 equiv of $[FeCp_2]^+$, producing a spectrum with bands at $\lambda_{max} = 640$ and 420 nm. These features are identical to those obtained for $[Mn^{IV}H_3buea(O)]^-$ at room temperature in DMSO.^{18a} Treating the solution with another equivalent of $[FeCp_2]^+$ generated a new spectrum containing peaks at λ_{max}/nm ($\epsilon_M/M^{-1} cm^{-1}$) = 820 (3600), 620 (3400), and 430 (10 000) that persisted for hours at -80 °C. We assign these features to the Mn^V –oxo complex $[Mn^VH_3buea(O)]$.

The oxidation of $[Mn^{III}H_3buea(O)]^{2-}$ by $[FeCp_2]^+$ was also studied using parallel (||)- and perpendicular (\perp)-mode EPR spectroscopy. $[Mn^{III}H_3buea(O)]^{2-}$ exhibited no signals in \perp -mode but showed a six-line hyperfine pattern ($A_z = 280$ MHz, 10 mT) in ||-mode at $g = 8.08$ (Figure 4A), which is

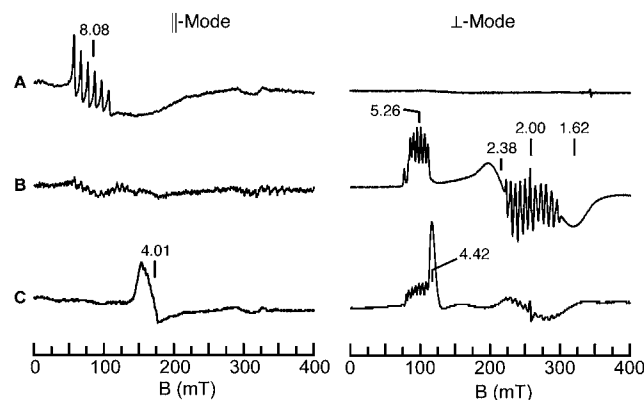


Figure 4. (left) ||- and (right) \perp -mode EPR spectra of (A) $[Mn^{III}H_3buea(O)]^{2-}$ and (B, C) after addition of (B) ~ 1 and (C) ~ 3 equiv of $[FeCp_2]^+$. The peak at $g = 4.42$ in the \perp -mode spectrum in (C) is from excess $[FeCp_2]^+$. Experimental conditions: temperature, 10 K; microwave frequency, 9.29 (||) or 9.62 (\perp) GHz.

indicative of an $S = 2$ spin state.¹⁹ One-electron oxidation of $[Mn^{III}H_3buea(O)]^{2-}$ was evident by the loss of the $g = 8.08$ signal in the ||-mode EPR spectrum and the appearance of features at $g = 5.26$, 2.38, and 1.62 in the \perp -mode spectrum (Figure 4B). These signals are associated with $[Mn^{IV}H_3buea(O)]^-$, as reported previously.^{18a} The relative signal intensities of $[Mn^{III}H_3buea(O)]^{2-}$ and simulations of the Mn^{IV} –oxo spectrum showed that 80% of the manganese in the sample was

converted to $[\text{Mn}^{\text{IV}}\text{H}_3\text{buea}(\text{O})]^-$. The 11-line hyperfine pattern centered at $g = 2$ is proposed to originate from a minority mixed-valent species (<1% in manganese).

Further oxidation of the sample produced a new \parallel -mode signal centered at $g = 4.01$ (Figure 4C),²⁰ which displayed a six-line hyperfine splitting of 113 MHz (4 mT) (Figure 3B). The position of the signal is indicative of a transition from the 11^\pm doublet of an $S = 1$ spin manifold^{20,21} and, taken together with the hyperfine splitting, is consistent with a monomeric Mn^{V} species that is assigned to $[\text{Mn}^{\text{V}}\text{H}_3\text{buea}(\text{O})]$. Simulations of this signal indicated that 60% of the initial Mn^{III} -oxo species was converted to $[\text{Mn}^{\text{V}}\text{H}_3\text{buea}(\text{O})]$.

Additional support for the $S = 1$ spin state for $[\text{Mn}^{\text{V}}\text{H}_3\text{buea}(\text{O})]$ came from Mn $K\beta$ X-ray emission spectroscopy (XES). Figure 5A shows the Mn $K\beta$ emission spectra of

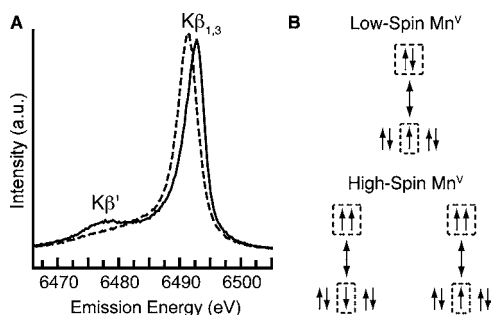


Figure 5. (A) Mn $K\beta$ XES spectra of $[\text{Mn}^{\text{V}}\text{H}_3\text{buea}(\text{O})]$ (solid) and the low-spin oxomanganese(V) complex $[\text{Mn}^{\text{V}}\text{DMB}(\text{O})]^-$ (dashed) collected at 10 K with an excitation energy of 10.0 keV. (B) Schematic diagrams of the 3d–3p exchange interactions in low- and high-spin Mn^{V} systems.

$[\text{Mn}^{\text{V}}\text{H}_3\text{buea}(\text{O})]$ and the low-spin oxomanganese(V) complex $[\text{Mn}^{\text{V}}\text{DMB}(\text{O})]^-$ (where DMB is a tetraamido macrocyclic ligand)^{12b} recorded at 10 K. The low-spin oxomanganese(V) spectrum shows a single peak ($K\beta_{1,3}$) at 6489.06 eV, while the spectrum of $[\text{Mn}^{\text{V}}\text{H}_3\text{buea}(\text{O})]$ is split into two peaks, $K\beta_{1,3}$ at 6490.50 eV and its satellite peak ($K\beta'$) at ~6476 eV. The $K\beta_{1,3}$ peak of $[\text{Mn}^{\text{V}}\text{H}_3\text{buea}(\text{O})]$ is shifted to higher energy by 1.44 eV relative to that of $[\text{Mn}^{\text{V}}\text{DMB}(\text{O})]^-$.

$K\beta$ XES detects the X-ray emission from the relaxation of a 3p electron into a 1s hole created by excitation of a 1s electron. The energy splitting in $K\beta$ spectra is caused by the exchange interaction between 3p and 3d orbitals.²² Two final states ($K\beta_{1,3}$ and $K\beta'$) exist because of constructive ($K\beta_{1,3}$) and destructive ($K\beta'$) spin-exchange interactions between the unpaired electrons in the 3p and 3d orbitals (Figure 5B). The $K\beta$ spectrum is thus sensitive to the effective number of unpaired 3d electrons and has been used to determine the Mn oxidation states in synthetic complexes and the OEC.²³ Energy shifts of the $K\beta_{1,3}$ peak was observed previously between low- and high-spin Fe^{III} species:²⁴ a shift of ~0.7 eV for the $K\beta_{1,3}$ peak position between the low- and high-spin species was found, and for the low-spin complex, the $K\beta'$ peak moved toward and merged into the low-energy side of the $K\beta_{1,3}$ line because of a decrease in valence spin. Analogous trends were observed in the $K\beta$ XES spectra of $[\text{Mn}^{\text{V}}\text{H}_3\text{buea}(\text{O})]$ and $[\text{Mn}^{\text{V}}\text{DMB}(\text{O})]^-$, findings that are consistent with $[\text{Mn}^{\text{V}}\text{H}_3\text{buea}(\text{O})]$ having an $S = 1$ spin ground state.

To confirm the presence of the oxo ligand in $[\text{Mn}^{\text{V}}\text{H}_3\text{buea}(\text{O})]$, resonance Raman (rR) spectroscopy was performed ($\lambda_{\text{ex}} = 647.1$ nm, 77 K). The rR spectrum of $[\text{Mn}^{\text{V}}\text{H}_3\text{buea}(\text{O})]$

contained O-sensitive features at 737 and 754 cm^{-1} that were converted into a single feature at 715 cm^{-1} when the sample was prepared with H_2^{18}O (Figure 6). On the basis of this

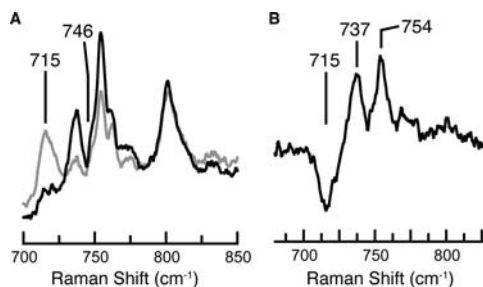
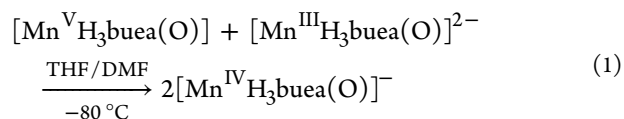


Figure 6. (A) Resonance Raman spectra of $[\text{Mn}^{\text{V}}\text{H}_3\text{buea}(\text{O})]$ (black) and $[\text{Mn}^{\text{V}}\text{H}_3\text{buea}(\text{O})]$ (gray) collected at 77 K with $\lambda_{\text{ex}} = 647.1$ nm and (B) the corresponding difference spectrum ($^{16}\text{O} - ^{18}\text{O}$).

behavior and the fact that none of the peaks were observed in rR spectra of the Mn^{III} or Mn^{IV} precursors,²⁵ we postulate that the two peaks in the ^{16}O sample constitute a Fermi doublet, a relatively common phenomenon in metal–oxygen compounds.²⁶ In support of the assignment of these features to a $\text{Mn}^{\text{V}}\text{–O}$ vibration, the observed difference of 31 cm^{-1} between the average position of the two peaks in the ^{16}O sample (746 cm^{-1}) and the 715 cm^{-1} peak in the ^{18}O sample agrees with the value expected on the basis of a harmonic $\text{Mn}^{\text{V}}\text{–O}$ oscillator [$\nu(\text{Mn}^{\text{V}}\text{–}^{16}\text{O})/\nu(\text{Mn}^{\text{V}}\text{–}^{18}\text{O}) = 1.043$; calcd = 1.046]. The $\text{Mn}^{\text{V}}\text{–O}$ vibration occurs at a slightly higher energy than that found by FTIR spectroscopy for $[\text{Mn}^{\text{IV}}\text{H}_3\text{buea}(\text{O})]$ [$\nu(\text{Mn}^{\text{IV}}\text{–O}) = 737$ cm^{-1}],^{18a} consistent with removal of the electron from orbitals not involved in $\text{Mn}^{\text{V}}\text{–O}$ bonding (Figure 2B). The $\text{Mn}^{\text{V}}\text{–O}$ vibration observed for $[\text{Mn}^{\text{V}}\text{H}_3\text{buea}(\text{O})]$ is similar to the $\nu(\text{Mn}^{\text{V}}\text{–O})$ of 759 cm^{-1} reported for a six-coordinate $\text{Mn}^{\text{V}}\text{–oxo}$ porphyrin complex; however, it is at significantly lower energy than those reported for non-porphyrinic low-spin oxomanganese(V) complexes. For example, the low-spin $[\text{Mn}^{\text{V}}\text{DMB}(\text{O})]^-$ complex has an $\text{Mn}^{\text{V}}\text{–O}$ vibration of 973 cm^{-1} .^{12b} This difference in vibrational energies reflects the disparate $\text{Mn}^{\text{V}}\text{–O}$ bond orders predicted for high- and low-spin oxomanganese(V) complexes (Figure 2) and the likelihood that the $\text{Mn}^{\text{V}}\text{–oxo}$ unit in $[\text{Mn}^{\text{V}}\text{H}_3\text{buea}(\text{O})]$ forms intramolecular H-bonds with the $[\text{H}_3\text{buea}]^{3-}$ ligand.

With the characterization of $[\text{Mn}^{\text{V}}\text{H}_3\text{buea}(\text{O})]$ we have now prepared oxomanganese complexes in three different oxidation levels that have similar primary and secondary coordination spheres. The chemistry within this series of complexes is currently under investigation, but the preliminary results are consistent with our spectroscopic findings that all are monomeric oxomanganese species. For instance, treating the newly discovered $[\text{Mn}^{\text{V}}\text{H}_3\text{buea}(\text{O})]$ complex with 1 equiv of $[\text{Mn}^{\text{III}}\text{H}_3\text{buea}(\text{O})]^{2-}$ produced 2 equiv of $[\text{Mn}^{\text{IV}}\text{H}_3\text{buea}(\text{O})]$, as determined by EPR and optical spectroscopies (Figure S2). This reaction is consistent with the comproportionation reaction described by eq 1:



Our work has further shown that changes in spin state within the series can be monitored with EPR spectroscopy, illustrating the utility of using \parallel -mode methods to probe integer-spin

states. In addition, we have obtained the first high-spin manganese(V) EPR and XES spectra, which can now be used as references in the study of other high-valent manganese systems, such as those that may be present in the OEC of PSII. These results also establish the viability of high-spin oxomanganese(V) species as possible reactive intermediates in a variety of chemical processes.

■ ASSOCIATED CONTENT

■ Supporting Information

Experimental details for all chemical reactions and measurements and figures for comproportionation reactions and electrochemical experiments. This material is available free of charge via the Internet at <http://pubs.acs.org>.

■ AUTHOR INFORMATION

Corresponding Author

aborovik@uci.edu

■ ACKNOWLEDGMENTS

The authors thank the NIH (GM50781 to A.S.B.; GM77387 to M.P.H.; GM47365 to W.B.T.; and GM55302 to V.K.Y.) and the Office of Science, Office of Basic Energy Sciences (OBES), Division of Chemical Sciences, Geosciences and Biosciences, Department of Energy (DOE) under Contract DE-AC02-05CH11231 (to V.K.Y. and J.Y.) for financial support. Portions of this research were carried out at the Stanford Synchrotron Radiation Lightsource (SSRL) operated by DOE, OBES. We thank Drs. J. Kern, R. A. Mori, and T.-C. Weng for their help during the XES data collection and Professor T. J. Collins for providing $[\text{NEt}_4][\text{Mn}^{\text{V}}\text{DMB}(\text{O})]$.

■ REFERENCES

- (1) (a) Groves, J. T.; Han, Y.-Z. In *Cytochrome P-450: Structure, Mechanism, and Biochemistry*, 2nd ed.; Ortiz de Montellano, P. R., Ed.; Plenum Press: New York, 1995; pp 3–48. (b) Holm, R. H. *Chem. Rev.* **1987**, *87*, 1401. (c) Gardner, K. A.; Kuehnert, L. L.; Mayer, J. M. *Inorg. Chem.* **1997**, *36*, 2069.
- (2) Meyer, T. J.; Nuynh, M. H. V.; Thorp, H. H. *Angew. Chem., Int. Ed.* **2007**, *46*, 5284.
- (3) Umena, Y.; Kawakami, K.; Shen, J.-R.; Kamiya, N. *Nature* **2011**, *473*, 55.
- (4) (a) McEvoy, J. P.; Brudvig, G. W. *Chem. Rev.* **2006**, *106*, 4455. (b) Cady, C. W.; Crabtree, R. H.; Brudvig, G. W. *Coord. Chem. Rev.* **2008**, *252*, 444.
- (5) (a) Kim, S. H.; Park, H.; Seo, M. S.; Kubo, M.; Ogura, T.; Klajn, J.; Gryko, D. T.; Valentine, J. S.; Nam, W. *J. Am. Chem. Soc.* **2010**, *132*, 14030. (b) Gao, Y.; Åkermark, T.; Liu, J.; Sun, L.; Åkermark, B. *J. Am. Chem. Soc.* **2009**, *131*, 8726.
- (6) Groves, J. T.; Lee, J.; Marla, S. S. *J. Am. Chem. Soc.* **1997**, *119*, 6269.
- (7) (a) Jin, N.; Groves, J. T. *J. Am. Chem. Soc.* **1999**, *121*, 2923. (b) Song, W. J.; Seo, M. S.; George, S. D.; Ohta, T.; Song, R.; Kang, M.-J.; Tosha, T.; Kitagawa, T.; Solomon, E. I.; Nam, W. *J. Am. Chem. Soc.* **2007**, *129*, 1268.
- (8) Gross, Z.; Golubkov, G.; Simkhovich, L. *Angew. Chem., Int. Ed.* **2000**, *39*, 4045.
- (9) Prokop, K. A.; de Visser, S. P.; Goldberg, D. P. *Angew. Chem., Int. Ed.* **2010**, *49*, 5091.
- (10) Jacobsen, E. N.; Zhang, W.; Muci, A. R.; Ecker, J. R.; Deng, L. *J. Am. Chem. Soc.* **1991**, *113*, 7063.
- (11) (a) Ballhausen, C. J.; Gray, H. B. *Inorg. Chem.* **1962**, *1*, 111. (b) Mayer, J. M. *Commun. Inorg. Chem.* **1988**, *8*, 125. (c) Winkler, J. R.; Gray, H. B. *Struct. Bonding (Berlin)* **2012**, *142*, 17.
- (12) (a) Collins, T. J.; Powell, R. D.; Slebonick, C.; Uffelman, E. S. *J. Am. Chem. Soc.* **1990**, *112*, 899. (b) Workman, J. M.; Powell, R. D.; Procyk, A. D.; Collins, T. J.; Bocian, D. F. *Inorg. Chem.* **1992**, *31*, 1548. (c) Lansky, D. E.; Mandimutsira, B.; Ramdhanie, B.; Clausen, M.; Penner-Hahn, J.; Zvyagin, S. A.; Telsler, J.; Krzystek, J.; Zhan, R.; Ou, Z.; Kadish, K. M.; Zakharov, L.; Rheingold, A. L.; Goldberg, D. P. *Inorg. Chem.* **2005**, *44*, 4485.
- (13) Groves, J. T.; Kruper, W. J.; Haushalter, R. C. *J. Am. Chem. Soc.* **1980**, *102*, 6375.
- (14) Zdilla, M. J.; Dexheimer, J. L.; Abu-Omar, M. M. *J. Am. Chem. Soc.* **2007**, *129*, 11505.
- (15) Mayer, J. M.; Thorn, D. L.; Tulip, T. H. *J. Am. Chem. Soc.* **1985**, *107*, 7454.
- (16) For examples of high-spin oxochromium(IV) complexes, see: (a) Hess, A.; Hörz, M. R.; Liable-Sands, L. M.; Lindner, D. C.; Rheingold, A. L.; Theopold, K. H. *Angew. Chem., Int. Ed.* **1999**, *38*, 166. (b) Qin, K.; Incarvito, C. D.; Rheingold, A. L.; Theopold, K. H. *J. Am. Chem. Soc.* **2002**, *124*, 14008.
- (17) Borovik, A. S. *Acc. Chem. Res.* **2005**, *38*, 54.
- (18) (a) Parsell, T. H.; Behan, R. K.; Hendrich, M. P.; Green, M. T.; Borovik, A. S. *J. Am. Chem. Soc.* **2006**, *128*, 8728. (b) Parsell, T. H.; Yang, M.-Y.; Borovik, A. S. *J. Am. Chem. Soc.* **2009**, *131*, 2762.
- (19) Hendrich, M. P.; Debunner, P. *Biophys. J.* **1989**, *56*, 489.
- (20) A total of 3 equiv of $[\text{FeCp}_2]^+$ was used to ensure complete oxidation at -80°C (see Figure 4C).
- (21) Details of this spectrum will be discussed in a forthcoming report.
- (22) (a) Tsutsumi, K.; Nakamori, H.; Ichikawa, K. *Phys. Rev. B* **1976**, *13*, 929. (b) Thole, B. T.; Cowan, R. D.; Sawatzky, G. A.; Fink, J.; Fuggle, J. C. *Phys. Rev. B* **1985**, *31*, 6856.
- (23) (a) Messinger, J.; Robblee, J. H.; Bergmann, U.; Fernandez, C.; Glatzel, P.; Visser, H.; Cinco, R. M.; McFarlane, K. L.; Bellacchio, E.; Pizarro, S. A.; Cramer, S. P.; Sauer, K.; Klein, M. P.; Yachandra, V. K. *J. Am. Chem. Soc.* **2001**, *123*, 7804. (b) Glatzel, P.; Bergmann, U. *Coord. Chem. Rev.* **2005**, *249*, 65.
- (24) Wang, X.; Randall, C. R.; Peng, G.; Cramer, S. P. *Chem. Phys. Lett.* **1995**, *243*, 469.
- (25) O-sensitive peaks were not observed in rR spectra for independently prepared samples of $[\text{Mn}^{\text{III}}\text{H}_3\text{buea}(\text{O})]^{2-}$ and $[\text{Mn}^{\text{IV}}\text{H}_3\text{buea}(\text{O})]^-$ that were collected under the same experimental conditions. Spectra were also collected for $[\text{Mn}^{\text{IV}}\text{H}_3\text{buea}(\text{O})]^-$ with $\lambda_{\text{ex}} = 457.9$ and 488.0 nm, and no O-isotope sensitive peaks were observed, indicating that the observed peaks in the rR spectra of the Mn^{V} species originated exclusively from $[\text{Mn}^{\text{V}}\text{H}_3\text{buea}(\text{O})]$.
- (26) (a) Holland, P. L.; Cramer, C. J.; Wilkinson, E. C.; Mahapatra, S.; Rodgers, K. R.; Itoh, S.; Taki, M.; Fukuzumi, S.; Que, L. Jr.; Tolman, W. B. *J. Am. Chem. Soc.* **2000**, *122*, 792. (b) Wilkinson, E. C.; Dong, Y.; Zang, Y.; Fujii, H.; Fraczkiewicz, R.; Fraczkiewicz, G.; Czernuszewicz, R. S.; Que, L. Jr. *J. Am. Chem. Soc.* **1998**, *120*, 955. (c) Namuswe, F.; Hayashi, T.; Jiang, Y.; Kasper, G. D.; Narducci Sarjeant, A. A.; Moënne-Loccoz, P.; Goldberg, D. P. *J. Am. Chem. Soc.* **2010**, *132*, 157.